J Appl Electrochem (2011) 41:609–616
DOI 10.1007/s10800-011-0269-0

ORIGINAL PAPER

Modelling of three-dimensional bipolar electrodes with irreversible reactions

O. González Pérez · J. M. Bisang

Received: 11 August 2010 / Accepted: 17 February 2011 / Published online: 2 March 2011

Abstract The behaviour of an electrochemical reactor with three-dimensional bipolar electrodes for irreversible reactions is analysed. Copper deposition at the cathodic side and oxygen evolution at the anodic one were adopted as test reactions at the bipolar electrode, from an electrolyte solution with a copper concentration lower than 1000 mg dm^{-3}, pH 2 and 1 M Na_2SO_4 as supporting electrolyte. A mathematical model considering the leakage current is proposed, which can represent the tendency observed in the experimental data related to cathodic thickness and potential at both ends of the bipolar electrode. High values of leakage current were determined, which restricts the faradaic processes to small thicknesses at both ends of the bipolar electrode. Likewise, the performance of the bipolar electrochemical reactor for the treatment of effluents is experimentally and theoretically examined. In this case, the conversion for copper removal was 90.1% after 480 min of operation with one bipolar electrode and 94.8% after 300 min of operation with two bipolar electrodes at a total current of 3 A.

Keywords Bipolar electrodes · Current distribution · Electrochemical reactors · Leakage current · Three-dimensional electrodes

List of symbols

A_s	Surface area per unit electrode volume (m^{-1})
C	Concentration (mol m^{-3}, mg dm^{-3})
CE	Current efficiency (%)
E	Electrode potential (V)
E_0	Reversible electrode potential (V)
E_0^0	Reversible electrode potential under standard conditions (V)
F	Faraday constant (C mol^{-1})
H	Electrode length (m)
i	Current density (A m^{-2})
$i_{b,F}$	Faradaic macrokinetic current density defined by Eq. 9 (A m^{-2})
I	Total current (A)
I^*	Leakage current (A)
j	Reaction rate (A m^{-2})
j_0	Exchange current density (A m^{-2})
j_L	Limiting current density (A m^{-2})
k_m	Mass-transfer coefficient (m s^{-1})
L	Thickness of the bipolar electrode (m)
Q	Volumetric flow rate (m^3 s^{-1})
RT/F	Constant (0.0261 V at 30 °C) (V)
S	Membrane area (m^2)
t	Time (s or min)
U	Cell voltage (V)
V_M	Reservoir volume (m^3)
V_R	Reactor volume (m^3)
W	Electrode width (m)
x	Axial coordinate (m)
y	Axial coordinate (m)
z	Axial coordinate (m)

Greek characters

α	Charge-transfer coefficient
β	Charge-transfer coefficient
ΔL	Thickness of the inert region of the bipolar electrode (m)
ε	Void fraction

O. González Pérez · J. M. Bisang (✉)
Programa de Electroquímica Aplicada e Ingeniería Electroquímica (PRELINE), Facultad de Ingeniería Química, Universidad Nacional del Litoral, Santiago del Estero 2829, S3000AOM Santa Fe, Argentina
e-mail: jbisang@fiq.unl.edu.ar

v_e Charge number of the electrode reaction
ρ Effective resistivity (Ω m)
ρ° Electrolyte resistivity (Ω m)
ψ By-passed fraction of the total current $= I^*/I$
τ_M Reservoir residence time $= V_M/Q$ (s)
τ_R Reactor residence time $= \varepsilon V_R/Q$ (s)

Subscripts

a Anodic
c Cathodic
exp Experimental
F Faradaic
i Reactor inlet
m Metal phase
mean Mean value
o Reactor outlet
s Solution phase
SCE Saturated Calomel Electrode
th Theoretical

1 Introduction

Several electrochemical reactions, such as the removal of contaminants from effluents and inorganic or organic electrosynthesis, take place at low current densities. Thus, three-dimensional electrodes are required to increase the space time yield of the reactor. It is suitable that the electrodes be arranged with a bipolar connection to provide a simple electrical setup, which facilitates easy maintenance. Additionally, this configuration has the advantage of using energy in a more economical way. However, the main drawback of the bipolar connection is the presence of leakage current [1], flowing through the pores of the three-dimensional electrode. Leakage current cannot be avoided but it can be minimized by an appropriate design of the reactor, which claims for the development of mathematical algorithms to calculate these devices and their experimental corroboration.

Relatively little work has been done on modelling three-dimensional bipolar electrodes. Alkire [2] presented a theoretical study of porous bipolar electrodes, which are considered to be the overlapping of two continua: the solution phase and the metal phase. However, the effect of the leakage current has been disregarded. In [3] the model has been extended to bipolar trickle bed reactors. Cheng et al. [4] reported the modelling of potentials, concentrations and current densities for flow through porous electrodes with monopolar or bipolar electric connections. For the removal of Pb(II) ions the monopolar system showed the best performance due to the leakage currents in the bipolar arrangement. In a previous paper [5] from this laboratory an exhaustive state of the art related to three-dimensional bipolar electrodes was given and a mathematical model was proposed to represent these devices when only one reversible electrochemical reaction occurs, as the deposition-dissolution of a metal. However, in the industrial practice the anodic and the cathodic sides of the bipolar electrode generate different products [4, 6, 7]. Therefore, the aim of the present paper is to extend the previous mathematical model considering the leakage current when irreversible reactions take place at the bipolar electrode. Two types of experiments were performed. In the first one, the main objective was to determine the active region in the electrode at constant concentration. In the second type, the removal of copper from dilute solutions was studied in order to examine the performance of three-dimensional bipolar electrodes for the processing of effluents.

2 Mathematical modelling

Figure 1a sketches an electrochemical reactor with a three-dimensional bipolar electrode consisting of three regions, i.e. the cathodic side, the anodic side and the inert region, where only the leakage current flows in the solution phase.

Assuming the metal phase as isopotential, the electrode potential at the axial position y is given by

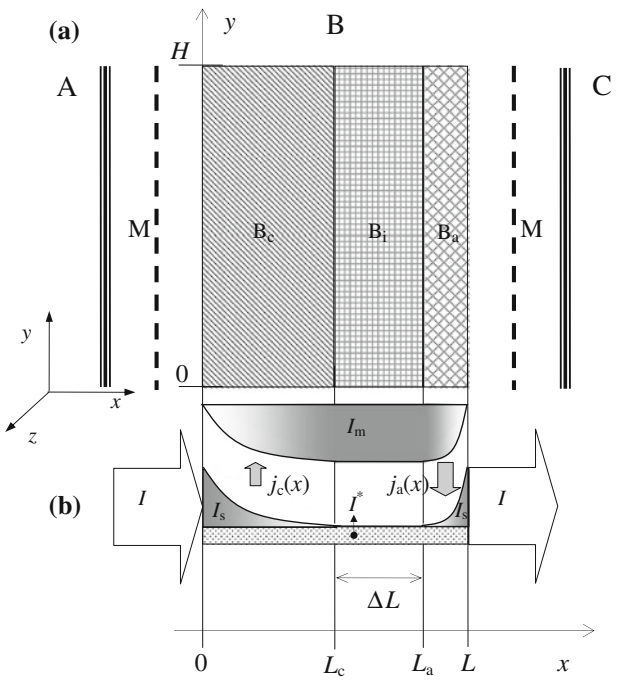

Fig. 1 **a** Diagram of an electrochemical stack with one bipolar three-dimensional electrode. A terminal anode, B bipolar electrode, B_a anodic side, B_c cathodic side, B_i inert region of the bipolar electrode, C terminal cathode, and M separators. **b** Schematic representation of the current variations in the metal and solution phases inside the bipolar electrode

$$\frac{d^2E(x)}{dx^2} = \rho_s A_s j(x) \tag{1}$$

with the boundary conditions

$$\text{at } x = 0 \quad \left.\frac{dE}{dx}\right|_{x=0} = \rho_s \frac{I}{S} \tag{2}$$

$$\text{at } x = L \quad \left.\frac{dE}{dx}\right|_{x=L} = \rho_s \frac{I}{S} \tag{3}$$

For the kinetics at the cathodic side a combined diffusion and charge-transfer expression, typical of metal deposition, is adopted according to

$$j(x) = \frac{\exp\left\{\frac{\nu_{e,c}F}{RT}\left[E(x) - E_{0,c}\right]\right\} - 1}{\exp\left\{\frac{\beta_c F}{RT}\left[E(x) - E_{0,c}\right]\right\}/j_{0,c} - 1/j_{L,c}} \tag{4}$$

Being

$$j_{L,c} = -\nu_{e,c}Fk_m C \tag{5}$$

And for the kinetics at the anodic side a Butler–Volmer equation, typical of gas evolution, given by

$$j(x) = j_{0,a}\left\langle \exp\left\{\frac{\alpha_a F}{RT}\left[E(x) - E_{0,a}\right]\right\} - \exp\left\{-\frac{\beta_a F}{RT}\left[E(x) - E_{0,a}\right]\right\}\right\rangle \tag{6}$$

is assumed. Thus, j is negative for the cathodic part and positive for the anodic one.

Figure 1b shows the current distribution along the electrode thickness in both phases and the flow of current. The current balance in the solution phase is

$$\frac{di_s(x)}{dx} = A_{s,k} j_k(x) \tag{7}$$

where k represents the anodic or the cathodic side of the bipolar electrode. Integrating Eq. 7 at the cathodic side results in

$$I_F = I - I^* = -SA_{s,c}\int_0^{L_c} j_c(x)\, dx \tag{8}$$

Thus, the faradaic macrokinetic current density at the cathodic side of the bipolar electrode is defined as

$$i_{b,F} = -A_{s,c}\int_0^{L_c} j_c(x)\, dx \tag{9}$$

Analogously, the faradaic current at the anodic side is

$$I_F = I - I^* = SA_{s,a}\int_{L_a}^{L} j_a(x)\, dx \tag{10}$$

being I^* the leakage current, which by-passes the bipolar electrode. Between the cathodic and anodic zones there is an inactive region where only the leakage current flows, which is given by

$$I^* = \frac{S}{\rho_s}\left.\frac{dE}{dx}\right|_{\text{inactive region}} \tag{11}$$

Taking into account that the slope of the electrode potential is constant in the inactive region is

$$I^* = \frac{S\left(E_{0,a} - E_{0,c}\right)}{\rho_s \Delta L} \tag{12}$$

Figure 2 shows an electrochemical reactor whose bipolar compartment is associated with a reservoir. The temporary behaviour of the bipolar compartment according to the plug flow model is given by

$$\tau_R \frac{\partial C(t,y)}{\partial t} = -\frac{H\partial C(t,y)}{\partial y} - \frac{i_{b,F}(t,y)WH}{Q\nu_{e,c}F} \tag{13}$$

The mass-balance in the reservoir yields

$$\tau_M \frac{dC_i(t)}{dt} = C_o(t) - C_i(t) \tag{14}$$

For $\tau_R \to 0$, Eq. 13 is simplified to

$$\frac{dC(t,y)}{dy} = -\frac{i_{b,F}(t,y)W}{Q\nu_{e,c}F} \tag{15}$$

Integrating Eq. 15 yields

$$C_o(t) = C_i(t) - \frac{W}{Q\nu_{e,c}F}\int_0^H i_{b,(F}(t,\, y)dy \tag{16}$$

Combining Eqs. 14 and 16 is

$$\frac{dC_i(t)}{dt} = -\frac{W}{V_M \nu_{e,c}F}\int_0^H i_{b,F}(t,\, y)dy \tag{17}$$

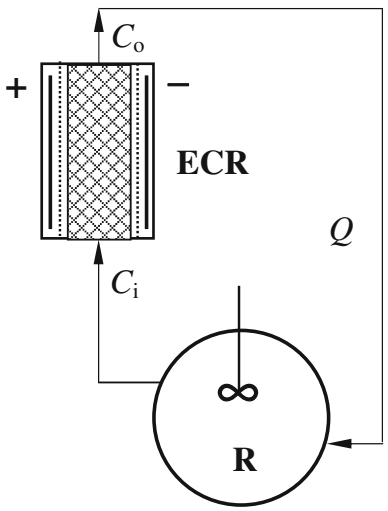

Fig. 2 Experimental arrangement of an electrochemical reactor associated with a reservoir

However, when the length of the reactor is small the conversion per pass is low and it is not necessary to take into account the concentration variation with the axial position y. Then, Eq. 17 is simplified to

$$\frac{dC_i(t)}{dt} = -\frac{I_F(t)}{V_M v_{e,c} F} \quad (18)$$

The simultaneous and iterative solution of Eqs. 1–12 allows for the calculation of the potential and current distribution, faradaic current and leakage current for a three-dimensional bipolar electrode. When the removal of copper from dilute solutions was studied, the theoretical value of copper concentration in the reservoir was obtained from Eq. 18. These calculations were performed by using the finite difference method. Table 1 summarizes the physicochemical properties and kinetic parameters used in the calculations, which in the case of copper deposition were taken from literature [8], and as to oxygen evolution they were determined in an additional experiment using a strand of the expanded metal electrode as an anode. The mass-transfer coefficient was calculated according to the correlation of Storck et al. [9], and the reversible electrode potential was evaluated by the Nernst equation with an activity coefficient calculated with the procedure of Kusik and Meissner [10].

3 Experimental

The experiments were performed in a flow-by electrochemical reactor made up of three compartments. The external compartments contain the terminal electrodes and the one in the middle, one or two bipolar electrodes. The terminal electrodes were made of ten segments of nickel positioned near the separator and inclined 30° from the vertical to deviate the gases to the backside of the electrodes. A calibrated resistor made from constantan wire, 100 mm long, 1.5 mm diameter and approximately 0.02 Ω resistance, was intercalated between the backside of each segment and the current feeder of the terminal electrode. By measuring the ohmic drop in the corresponding resistor, it was possible to determine the axial current distribution at each terminal electrode. The projected area of each segment on the separator was 1 × 5 cm^2 and the backside of each segment was covered with epoxy resin to make it non-conductive. The data acquisition was performed with an analogue multiplexer commanded by a computer. The influence of these resistors on the cell voltage is negligible due to the small value of its resistance.

Table 1 Physicochemical properties and kinetic parameters used in modelling

ρ° (Ω m)	9.5×10^{-2}
$E_{0,a}$ (V vs. SCE)	0.8685
$E^0_{0,c}$ (V vs. SCE)	0.1
$j_{0,a} A_{s,a}$ (A m^{-3})	4.12
$j_{0,c}$ (A m^{-2})	$1.13 \times 10^{-2}\ C^{0.82}$(mg dm^{-3})
α_a	0.65
β_a	1.35
β_c	0.36
$v_{e,c}$	2

The dimensions of the bipolar compartment were 50 mm wide, 100 mm high and 17 mm thick and it was separated from the terminal electrodes by cationic exchange membranes. The cathodic part of the bipolar electrode was a stack of nets fabricated from rectangular plates, 50 mm × 100 mm, which were welded at several points in the perimeter to obtain mechanical stability of the structure and to ensure isopotentiality of the metal phase. It was made from a 304 stainless steel woven-wire mesh, 50 mesh size (0.177 mm wire diameter and 0.331 mm distance between wires). The average value of the geometric specific surface area was approximately 6420 m^{-1} with a void fraction of 0.70. In the experiments with one bipolar electrode the thickness of the cathodic side was 15 mm, and 6 mm for each cathodic side when two bipolar electrodes were used. These were separated by two plastic nets, each 0.5 mm thick, whose geometric characteristics were similar to the stainless steel meshes to avoid the by-pass of the electrolyte through the separator. The anodic part of the bipolar electrodes was a sheet of flattened expanded titanium coated with RuO_x (DSA), 2 mm thick.

The experiments were carried out galvanostatically, at 30 °C, and two saturated calomel electrodes were used as reference, each being connected to Haber-Luggin capillaries positioned at both sides of the bipolar compartment.

Owing to the special construction of this reactor, the primary current distribution is uniform. Likewise, to achieve more uniform mass-transfer conditions along the reactor, flow distributor plates with 149 holes, 1.5 mm in diameter, were arranged in the inlet and outlet of the electrolyte in each compartment. The reactor was made part of two flow circuits, one for the terminal electrodes and the second circuit for the bipolar compartment. Each flow circuit comprised a pump, a flow meter and connections to maintain the temperature at the preset value, 30 °C.

The electrolyte solution in the bipolar electrodes was 1 M Na_2SO_4 and H_2SO_4, to obtain pH 2, with a copper concentration lower than 1000 mg dm^{-3}. Copper deposition takes place at the cathodic side and oxygen evolution at the anodic side of the bipolar electrode. During the experiment, samples of solution were taken from the reservoir at regular intervals to determine the copper concentration by atomic absorption spectroscopy. In the

experiments to examine current distribution only one bipolar electrode was used, and a known volume of saturated $CuSO_4$ solution was added to the reservoir to maintain the concentration in the preset value. The reservoir volume for the bipolar compartment was 10 dm^3. A solution of 1 M NaOH, 2.5 dm^3, was used in the terminal compartments. Hydrogen and oxygen evolution were the cathodic and anodic reactions at the terminal electrodes.

During the experiments, the axial current distribution at the terminal electrodes was measured. After the experiments, cross-sections of the cathodic side of the bipolar electrodes, embedded in epoxy resin, were examined with a metallurgical microscope to determine the active region and the thickness distribution of the deposit.

The leakage current was experimentally determined as the difference between the total current and the current used for copper deposition, which was calculated from the mass of copper deposited at the cathode.

The oxygen concentration in the reservoir was determined by the Winkler method [11], which was in the range from 2.73 to 3.39 mg dm^{-3} in accordance with the oxygen solubility in this electrolyte, 3.54 mg dm^{-3}, calculated with the procedure outlined in [12]. Thus, the reduction of oxygen was disregarded as a secondary reaction at the cathodic side of the bipolar electrode due to its low concentration in comparison with copper concentration. Further details related to the construction of the equipment, data acquisition of current distribution and experimental procedure are given in our previous work [5].

4 Results and discussion

Figure 3 shows the current distribution at the terminal electrodes as a function of the axial position y for different total currents and volumetric flow rates. The vertical bar represents the standard error of the mean. It can be observed that the axial current distribution is uniform at both terminal electrodes.

Table 2 summarizes the main conditions of the experimental results. Column 7 shows that the by-passed fraction of the total current is very high in comparison with the values reported in the previous work [5], where the anodic reaction was the dissolution of copper. It must be emphasized that the current in the bipolar electrode can flow in two parallel paths. The first one is the faradaic current and in the second path the current flows through the pores of the three-dimensional electrode, called leakage current. In case that the reversible cell voltage is high the potential difference applied to the bipolar electrode increases, and for a given value of total current the leakage current is enlarged whereas the faradaic current diminishes. When copper deposition as cathodic reaction and oxygen

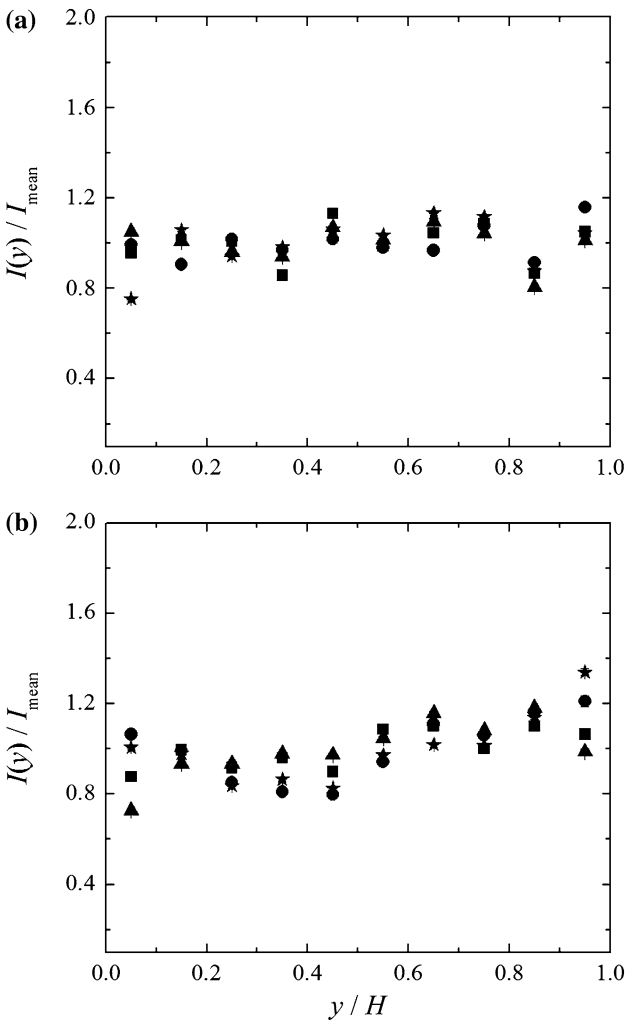

Fig. 3 Current distribution as a function of the axial position y. One bipolar electrode. **a** Terminal anode; **b** Terminal cathode. *Filled square*: $I = 2.0$ A, $C_{mean} = 1015$ mg dm^{-3}, $Q = 6.0 \times 10^{-6}$ m^3 s^{-1}; *filled circle*: $I = 3$ A, $C_{mean} = 382$ mg dm^{-3}, $Q = 6.0 \times 10^{-6}$ m^3 s^{-1}; *filled triangle*: $I = 3.0$ A, $C_{mean} = 472$ mg dm^{-3}, $Q = 1.97 \times 10^{-5}$ m^3 s^{-1}; *filled star*: $I = 3.0$ A, C ranged from 604 to 60 mg dm^{-3}, $Q = 1.97 \times 10^{-5}$ m^3 s^{-1}. *Vertical bars*: standard error of the mean

evolution as anodic reaction take place in the bipolar electrode, the reversible cell voltage is approximately 0.85 V. Thus, it is necessary to apply to the bipolar electrode a potential difference higher than the last value to produce the faradaic processes. This high potential difference generates an important leakage current, which produces a marked ohmic drop in the solution phase inside the bipolar electrode so that the faradaic processes only occur in a small thickness at both ends of the bipolar electrode, as reported in the third column of Table 3 for the cathodic thickness.

Figure 4 shows the cathodic thickness as a function of the z coordinate, electrode width, where it is observed that the copper deposition is lower at the borders of the electrode due to the different hydrodynamic conditions inside

Table 2 Summary of experimental data

Exp.	I (A)	t (min)	$Q \times 10^6$ ($m^3\ s^{-1}$)	U (V)	C_{mean} (mg dm^{-3}) or $C_{initial} - C_{final}$ (mg dm^{-3})	$\psi\|_{exp}$ (%)	$CE\|_{exp}$ (%)
1	2	350	6.0	5.51	1015	78.31	21.69
2	3	360	6.0	7.40	382	75.46	24.54
3	3	360	19.7	6.92	472	55.95	44.05
4	3	480	19.7	7.64	604–60	80.81	19.19
5[a]	3	300	19.7	8.99	439–23	87.73	12.27

[a] Two bipolar electrodes

Table 3 Comparison of theoretical and experimental results

Exp.	$\rho_{s,\ correlated}$ (Ω m)	$L_c\|_{mean,\ exp}$ (mm)	$L_c\|_{th}$ (mm)	$E(0)\|_{mean,\ exp}$ (V)	$E(0)\|_{th}$ (V)	$E(L)\|_{mean,\ exp}$ (V)	$E(L)\|_{th}$ (V)
1	0.254	2.04	1.63	−0.238	−0.137	1.116	1.236
2	0.196	5.61	2.86	−0.575	−0.285	1.230	1.250
3	0.266	3.82	2.93	−0.565	−0.321	1.286	1.267
4	0.23–0.16	6.31	2.83[a]	−0.411	−0.302[a]	1.201	1.311[a]

The potentials are referred against the saturated calomel electrode

[a] Mean values

the electrode. However, the deposition becomes more uniform at the z coordinate when the volumetric flow rate is increased.

The oxygen evolution at the anodic side of the bipolar electrode produces the formation of a bubble dispersion, which increases the effective electrolyte resistivity in a non-predictable way. Thus, in order to improve the agreement between the experimental results and the model, the mathematical treatment was solved using the effective resistivity as a fitting parameter, which was adjusted to obtain the gravimetric value of the current for copper reduction. As expected, the correlated effective resistivity, reported in the second column of Table 3, was always higher than the value used in the previous work [5], 0.16 Ω m, for a system without gas evolution. However, only a small improvement between experimental and theoretical data, related to cathodic thickness, was obtained from these calculations with higher values of effective resistivity.

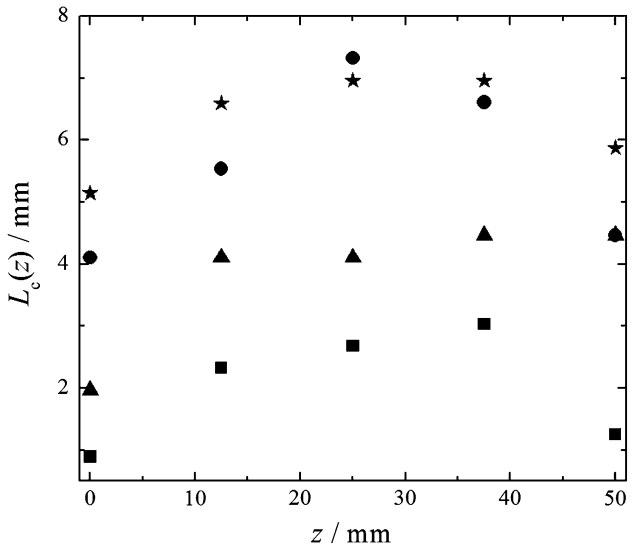

Fig. 4 Cathodic thickness as a function of the position at the electrode width. Symbols according to the legend of Fig. 3

The experimental and theoretical data related to cathodic thickness, and potential at both ends of the bipolar electrode are summarized in Table 3, where the experimental results correspond to mean values. Moreover, Fig. 5 shows the temporal response of the potential at both ends of the bipolar electrode for a typical experiment, while the full lines represent the theoretical model. It can be inferred that the theoretical model is able to characterize the tendency observed in the experimental results and that it corroborates the small values for the cathodic thickness. The discrepancy between the experimental and theoretical potentials at the cathodic end of the bipolar electrode can be explained taking into account that the experimental values were measured in only one point in the periphery of the electrode, where, according to Fig. 4, copper deposition takes place at lower current density.

The high value of leakage current also produces a diminution in the current efficiency as reported in the last column in Table 2. However, the current efficiency increases when the volumetric flow rate rises due to the enhancement of the mass-transfer conditions for copper deposition.

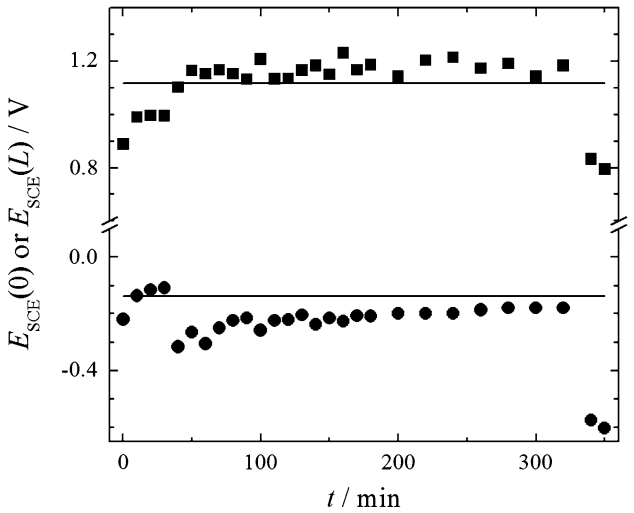

Fig. 5 Potential at both sides of the bipolar electrode as a function of time. $I = 2.0$ A, $C_{mean} = 1015$ mg dm^{-3}, $Q = 6.0 \times 10^{-6}$ m^3 s^{-1}. *Filled circle*: $E_{SCE}(0)$, cathodic side. *Filled square*: $E_{SCE}(L)$, anodic side. *Full lines*: theoretical behaviour

Figure 6 shows the change in concentration as a function of time for a typical experiment with one bipolar electrode to determine the performance of the reactor for the processing of effluents. Additional data of this experiment are given in the fourth row of Tables 2 and 3. A pronounced change of concentration is observed in the first stages of the experiment and then a slower decay takes place. The full line represents the theoretical behaviour according to the mathematical model assuming a linear decrease of the effective electrolyte resistivity with time. For that, at the beginning when the faradaic current is important, it was taken the mean value of the three experiments at constant copper concentration reported in the second column of Table 3, i.e. 0.23 Ω m, and 0.16 Ω m at the end of the experiment. This last value was calculated with the Bruggeman equation neglecting the gas evolution inside the electrode [5], because the oxygen generation is low at the end of the experiment. A close agreement between experimental and theoretical values can be seen. Table 2, in the last row, also reports that the use of two bipolar electrodes in the middle compartment produces an important change in concentration in the reservoir, 94.8% conversion after 300 min of operation, in spite of the low current efficiency as a consequence of the high leakage current due to the lower thickness of each electrode. However, this configuration showed a different amount of copper deposited at each bipolar electrode, which can be attributed to the accumulation of gases at the separator or to differences in the hydrodynamic behaviour inside the compartment. Thus, in this case it was difficult to correlate the experimental results.

According to Eq. 18 the current used for copper reduction can also be obtained from the slope of the concentration versus time experimental curve in the reservoir. Thus, Fig. 7 reports the by-passed fraction of current as a function of time, where an increase of the leakage current is observed with time. This is a consequence of the diminution in the copper concentration. The full line represents the behaviour according to the theoretical model, where a close agreement is observed with the experimental results. Figure 8 shows that the theoretical current efficiency decreases with time because of the increase in leakage current. The mean value of the theoretical current efficiency, dashed line, agrees with the gravimetric current efficiency experimentally determined.

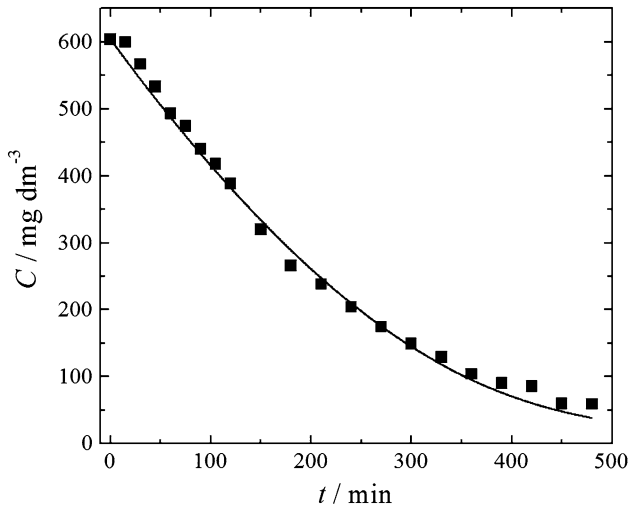

Fig. 6 Concentration as a function of time. One bipolar electrode. $I = 3$ A. $Q = 1.97 \times 10^{-5}$ m^3 s^{-1}. *Full line*: theoretical behaviour. $\rho_s(0) = 0.23$ Ω m and ρ_s (480 min) = 0.16 Ω m

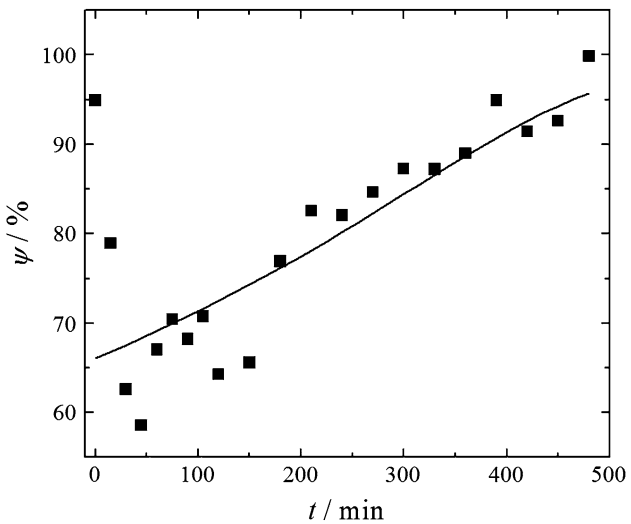

Fig. 7 By-passed current fraction as a function of time for the experiment reported in Fig. 6

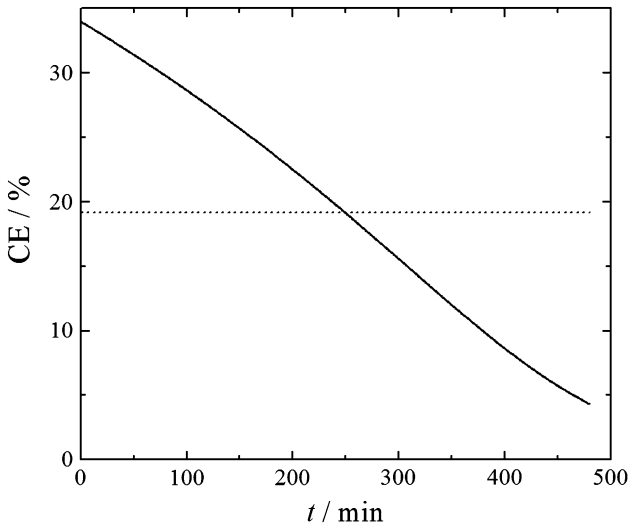

Fig. 8 Current efficiency as a function of time for the experiment reported in Fig. 6. *Full line* theoretical value, *dotted line* gravimetric determination

5 Conclusions

- When irreversible reactions take place in a three-dimensional bipolar electrode, the by-passed fraction of the total current is more important than when only a reversible electrochemical reaction occurs, as a consequence of the higher potential difference applied to the electrode. Therefore, it is convenient that the reversible potentials of the reactions at both sides of the bipolar electrode be close in order to minimize the by-passed fraction of current.
- The high leakage current generates that the electrochemical reactions only take place in small regions at the ends of the bipolar electrodes. Thus, an important part of the electrode becomes inactive.
- The high leakage current produces a diminution of the current efficiency.
- The mathematical model is reliable as it represents the tendency of the experimental results in a three-dimensional bipolar electrode working with irreversible reactions.
- An electrochemical reactor with bipolar three-dimensional electrodes presents a good performance for the processing of effluents. Also, this reactor offers as advantage simplified constructive features with respect to monopolar devices. However, it was corroborated that the main shortcoming of the bipolar connection is the presence of leakage current, flowing through the pores of the three-dimensional structure, which diminishes the current efficiency.

Acknowledgments This work was supported by the Agencia Nacional de Promoción Científica y Tecnológica (ANPCyT), Consejo Nacional de Investigaciones Científicas y Técnicas (CONICET) and Universidad Nacional del Litoral (UNL) of Argentina.

References

1. Pletcher D, Walsh FC (1993) Industrial electrochemistry, Chap. 2. Chapman and Hall, London, pp 136–141
2. Alkire R (1973) J Electrochem Soc 120:900
3. Fleischmann M, Ibrisagić Z (1980) J Appl Electrochem 10:151
4. Cheng CY, Kelsall GH, Pilone D (2005) J Appl Electrochem 35:1191
5. González Pérez O, Bisang JM (2010) J Appl Electrochem 40:709
6. Güvenç A, Tarik Pekel A, Mete Koçkar Ö (2004) Chem Eng J 99:257
7. Gupta N, Oloman CW (2006) J Appl Electrochem 36:255
8. Bisang JM (1996) J Appl Electrochem 26:135
9. Storck A, Robertson PM, Ibl N (1979) Electrochim Acta 24:373
10. Kusik CL, Meissner HP (1978) AIChE Symp Ser 74:14
11. APHA (1998) Standard methods for the examination of water and wastewater, 20th edn, APHA, AWWA, WEF, Washington DC, Part 4500, p 4.129
12. Tromans D (2000) Ind Eng Chem Res 39:805